SCIENCE CHINA
Earth Sciences

• RESEARCH PAPER •

February 2016 Vol.59 No.2: 307–319
doi: 10.1007/s11430-015-5140-4

Estimation of key surface parameters in semi-arid region and their impacts on improvement of surface fluxes simulation

LIU Ye[1], GUO WeiDong[1*] & SONG YaoMing[2]

[1] *Institute for Climate and Global Change Research, School of Atmospheric Sciences, Nanjing University, Nanjing 210093, China;*
[2] *College of Atmospheric Science, Nanjing University of Information Science and Technology, Nanjing 210044, China*

Received March 2, 2015; accepted May 19, 2015; published online July 21, 2015

Abstract Uncertainties in some key parameters in land surface models severely restrict the improvement of model capacity for successful simulation of surface-atmosphere interaction. These key parameters are related to soil moisture and heat transfer and phy- sical processes in the vegetation canopy as well as other important aerodynamic processes. In the present study, measurements of surface-atmosphere interaction at two observation stations that are located in the typical semi-arid region of China, Tongyu Station in Jilin Province and Yuzhong Station in Gansu Province, are combined with the planetary boundary layer theory to estimate the value of two key aerodynamic parameters, i.e., surface roughness length z_{0m} and excess resistance κB^{-1}. Multiple parameterization schemes have been used in the study to obtain values for surface roughness length and excess resistance κB^{-1} at the two stations. Results indicate that z_{0m} has distinct seasonal and inter-annual variability. For the type of surface with low-height vegetation, there is a large difference between the default value of z_{0m} in the land surface model and that obtained from this study. κB^{-1} demonstrates a significant diurnal variation and seasonal variability. Using the modified scheme for the estimation of z_{0m} and κB^{-1} in the land surface model, it is found that simulations of sensible heat flux over the semi-arid region have been greatly improved. These results suggest that it is necessary to further evaluate the default values of various parameters used in land surface models based on field measurements. The approach to combine field measurements with atmospheric boundary layer theory to retrieve realistic values for key parameters in land surface models presents a great potential in the improvement of modeling studies of surface-atmosphere interaction.

Keywords Semi-arid region, Turbulent transfer, Surface roughness length, Excess resistance, Field experiments

Citation: Liu Y, Guo W D, Song Y M. 2016. Estimation of key surface parameters in semi-arid region and their impacts on improvement of surface fluxes simulation. Sci China Earth Sci, 59: 307−319, doi: 10.1007/s11430-015-5140-4

1. Introduction

Arid and semi-arid regions occupy about 40% of the total land areas in the world (Verhoef et al., 1999). In China, arid and semi-arid region covers about 40% of the total land mass (Fu et al., 2005). Located in the transitional zone between the desert and moist climate and ecosystem, the arid and semi-arid region of China is highly sensitive to climate change in the context of global warming (Fu et al., 2002). Desertification in this region has become significant in recent years (Ma et al., 2003, 2005). Results of the Regional Climate Model Inter-comparison Project in Asia (RMIP) indicate that the largest bias in precipitation simulation almost always occurs in semi-arid regions of Asia (Fu et al., 2005; Zhang et al., 2005; Feng et al., 2007; Yao et al., 2010; Ling et al., 2012).

One important reason for the weakness of regional climate models in their simulations over the semi-arid region is the insufficient knowledge of the surface-atmosphere interaction in this area. With the advances in observational techniques and improvements in precision of measurement

*Corresponding author (email: guowd@nju.edu.cn)

instruments, field measurements and observations become more accurate and hence reliable for verification. Therefore, the differences between model results mainly arise from inappropriate model structures and physical parameters (Xie et al., 2005).

With the continuous development of land surface model, the physical parameterization scheme is being improved to better describe physical processes in the surface. More parameters are incorporated into the land surface model, which has already included a large number of parameters. The major parameters in land surface model include vegetation canopy parameters (e.g., leaf area index, fractional vegetation cover, stomatal resistance), soil parameters (e.g., soil porosity, saturated hydraulic conductivity), and aerodynamic parameters (e.g., surface roughness length, thermal transfer resistance) (Sun et al., 2005). These parameters are critical for the land surface model to successfully reproduce the realistic physical processes (Liu et al., 2004).

The surface heat flux, which is a critical variable in surface-atmosphere interaction, can serve as an important index to assess the capability of land surface model (Dan et al., 2011). The surface roughness length (z_{0m}, also named as aerodynamic roughness) and thermal transfer resistance (κB^{-1}) are two key parameters in the calculation of surface heat flux. From the perspective of the vertical wind profile in the boundary layer, the surface roughness length is defined as the height at which the wind speed becomes zero. Water and heat fluxes are exchanged between the surface and atmosphere through turbulent mixing process, and z_{0m} reflects the aerodynamic resistance of turbulent mixing and momentum, heat, and moisture transfers between the surface and the atmosphere. Pitman (2003) qualitatively summarized the effects of z_{0m} in the calculation of surface heat flux, suggesting that a decreased z_{0m} to a certain extent would lead to an increase in surface aerodynamic resistance and decreases in sensible and latent heat fluxes. In most of the land surface models currently used internationally, the sensible heat flux is calculated (by means of a 'resistance' approach) by considering the aerodynamic resistance. The sensible heat flux transfer is conceived to be a process analogous to the flow of electrical current. Hence, the sensible heat flux can be calculated using the temperature difference between the surface and air divided by the aerial resistance to the flow of sensible heat (Verhoef et al., 1997). The excess resistance parameter (κB^{-1}), is defined as: $\kappa B^{-1} = \ln(z_{0m} / z_{0h})$, Where z_{0m} and z_{0h} are the surface momentum and heat roughness length, respectively. z_{0h} represents the height at which the air temperature is the same as the surface temperature. The larger the κB^{-1} is, the larger the thermal aerial resistance will become, and the smaller the heat flux will be. The opposite is true for a smaller κB^{-1}. Therefore, the values of z_{0h} and κB^{-1} are directly linked to the calculation of the surface heat flux. Uncertainty in these two parameters significantly restricts the improvement in the model performance.

In addition, the model development history indicates that values of the key parameters in one specific model are often determined and verified based on a single station observations or results of several experiments. These values are then regarded as representative (default) values for these important parameters and applied in various land surface models (Sellers et al., 1986; Dickinson et al., 1993). Therefore, it is no wonder that when the land surface model is applied to regions other than where it is originally developed for, the key parameters in the model must be adjusted based on the specific characters of the study regions. The model performance and the reliability of the model simulations are largely dependent on the reasonable settings of these key parameters in the model.

In recent years, estimation of the surface roughness length has been investigated in many studies (Gao et al., 2002; Zhong et al., 2002; Zhang et al., 2003; Zhang et al., 2009). At the initial stage of model development, z_{0m} is often estimated based on the geometric height of barriers (Wieringa, 1993). Later Chen at al. (1997) proposed a method to estimate z_{0m} using the average wind speed and turbulence measured by ultrasonic anemometer. This method was verified for the meadow surface in the Tibetan Plateau (Ma et al., 2008). Since then, Takagi et al. (2003) proposed a method to calculate z_{0m} based on wind speed in the surface layer. Zhou et al. (2007) used this method to obtain the surface roughness length for the forest surface in Changbai Mountain. Yang et al. (2008) combined the similarity theory with statistical method to estimate the optimal z_{0m}, and calculated the surface roughness length for various surface types in arid and semi-arid regions. However, due to the limitation in sample size, differences in criteria for sample selection, and different statistical methods used in these studies, there exist large discrepancies in the results of z_{0m} estimation.

The semi-arid region of China is located in a zone of the farming-pastoral ecotone, where the grassland has severely degraded due to the influence of the significant drying trend in this area. Despite some progresses in the estimation of surface parameters and improvements in land surface models (Chen et al., 2010; Liu et al., 2012; Zeng et al., 2012; Zheng et al., 2012, 2014), seasonal and inter-annual variability of the surface roughness length in several typical surface types of grassland, farmland, and degraded grassland have not been well studied. Meanwhile, the reasonable application of the estimated parameters in land surface models has not been fully investigated. In this study, the long-term continuous measurements of surface-atmosphere interaction at two ground sites, Tongyu in Jilin Province and Yuzhong in Gansu Province, are combined with planetary boundary layer theory to calculate z_{0m} and κB^{-1}. The two observation stations are located at the east and west ends of the semi-arid region of China, respectively, and the measurements are conducted over farmland, grassland, and degrad-

ed grassland. Various methods are applied in the calculation. The inter-annual, seasonal, and diurnal variations of these two variables are analyzed. The observations from Tongyu and Yuzhong are first used to compare the performance of various parameterization schemes. The scheme that demonstrates the best performance is then identified and applied to the Common Land Model (CoLM) to investigate the impact of these improved parameters on the simulation of surface heat flux.

2. Data and methodology

2.1 Introduction of observation stations and data

Turbulent fluxes observed in the ground stations are a perquisite for the estimation of surface roughness length and excess resistance, which are two important parameters in land surface models. The observations used in the present study were obtained at Tongyu Station, which has a farmland site and a degraded grassland site, and from the ground station maintained by Semi-arid Climate Observatory and Laboratory (Yuzhong Station, here after SACOL) in Lanzhou University. Tongyu Station (44.42°N, 122.87°E) is located at Tongyu County, Baicheng, Jilin Province. It is one of the reference sites in the Coordinated Energy and Water Cycle Observation Project (CEOP). Tongyu Station is located in the semi-arid region of North China, where the annual total precipitation is about 404 mm (Fu et al., 2008). It consists of two observational sites that are located at farmland (Figure 1(a)) and degraded grassland (Figure1 (b)), respectively, with a distance of 5 km in between. The major crop grown in the farmland is corn, while sunflower is also grown. The growing season for crops in the farmland is from May to October. The height of crops in summer can reach up to 2 m, while the surface is bare soil in the non-growing season. The height of grass in the degraded grassland is about 10–20 cm in the summer, and below 5 cm in the winter and spring (Liu et al., 2004; Tu et al., 2009; Feng et al., 2012). Yuzhong Station (35.57°N, 104.08°E) is located at Yuzhong campus of Lanzhou University, which is characterized by semi-arid climate of Loess Plateau. Annual precipitation in Yuzhong is 381.8 mm, and the plants growing in Yuzhong include low round pteridophyllum, mugwort, Suaeda etc., which are low-height and drought tolerant grasses (Huang et al., 2008; Guan et al., 2008, 2009; Wang et al., 2010). Observation towers are set up at the above three sites to measure gradients of wind speed, temperature, and humidity. Surface observation systems are applied for measurement of the basic meteorological elements, including pressure, temperature, humidity, wind speed and direction in the surface layer, the upward and downward shortwave and long-wave radiation fluxes. The eddy-covariance system is used to obtain the sensible and latent heat fluxes as well as turbulent CO_2 flux. Soil observation includes soil temperature and moisture measurements at 0–80 cm and soil heat flux at the surface.

The eddy-covariance system measurements and observation tower measurements of gradients for the period 2003–2008 at Tongyu Station and for the period 2007–2008 at Yuzhong Station are used in the present study. Quality control has been performed for the turbulence measurements, including: (1) removal of invalid measurements, (2) calculation of turbulent fluxes with rotation of coordinates, (3) frequency response correction (Moore, 1986) and WPL correction (Webb et al., 1980), (4) quality control (Foken et al., 2004).

2.2 Calculation of surface roughness length (z_{0m}) and excess resistance (κB^{-1})

According to the Monin-Obukhov similarity theory, the revised wind profile in the surface layer can be expressed as:

$$u = \frac{u_*}{k}[\ln\frac{z_m - d}{z_{0m}} - \psi_m(\zeta)], \quad (1)$$

where u is the horizontal wind speed (m/s), k is the von Karman constant, which is set to be 0.4 in the present study, z_m is height of the instrument probe (m), d is the zero-plane

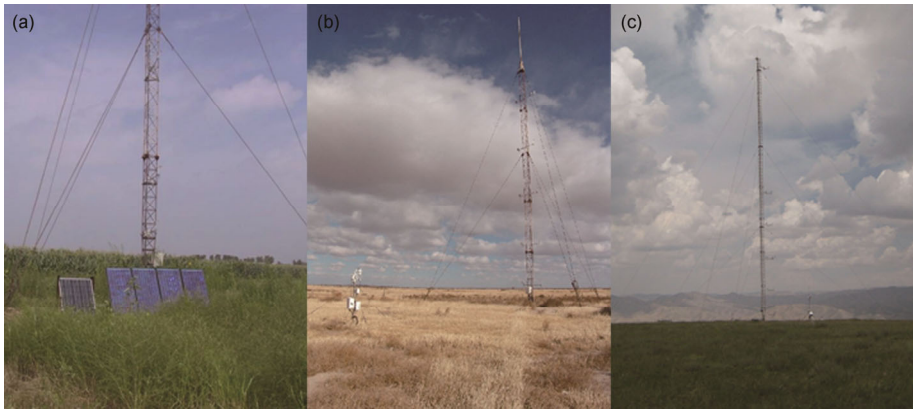

Figure 1 Tongyu Station farmland site (a), degraded grassland site (b), and overview of Yuzhong Station (c).

displacement, z_{0m} is the aerodynamic roughness length, u_* is the friction velocity (m s^{-1}). The stability parameter is given by $\zeta = z_m / L$, where L is the Obukhov length. The stability correction function $\psi_m(\zeta)$ can be expressed as (Dyer, 1974):

$$\begin{cases} \psi_m = 2\ln\left(\dfrac{1+x}{2}\right) + \ln\left(\dfrac{1+x^2}{2}\right) - 2\arctan x + \dfrac{\pi}{2}, & \zeta < 0 \\ \psi_m = -5\zeta, & \zeta > 0. \end{cases} \quad (2)$$

$$x = (1-16\zeta)^{1/4}. \quad (3)$$

The basic mechanisms for turbulence generation include mechanical and buoyancy. The mechanical turbulence is mainly determined by d and z_{0m}, while the buoyancy turbulence is largely determined by $\psi_m(\zeta)$. Therefore, the wind observations at three levels are used in the logarithmic wind profile equation under neutral condition to calculate zero-plane displacement using Newton's iterative method. The iterative equation is written as:

$$f(d) = \frac{u_1 - u_2}{u_1 - u_3} - \frac{\ln(z_1 - d) - \ln(z_2 - d)}{\ln(z_1 - d) - \ln(z_3 - d)}, \quad (4)$$

$$g(d) = d - \frac{f(d)}{f'(d)}. \quad (5)$$

The wind measurements at the three levels of z_1, z_2 and z_3 are used in the above equation. Iteration begins with a first guess of d until the objective function $g(d)$-d tends to zero and the value of d, the zero-plane displacement, can be determined. With the value of d available, u_* can be determined by iteration using wind and temperature measurements at two different levels. The method is described below:

$$u_* = k(u_2 - u_1) / \ln\left(\frac{z_2 - d}{z_1 - d}\right), \quad (6)$$

$$\theta_* = k(\theta_2 - \theta_1) / \ln\left(\frac{z_2 - d}{z_1 - d}\right), \quad (7)$$

$$L = -\frac{u^3_*}{k\frac{g}{\overline{\theta}}\overline{w'\theta'}} = \frac{u^2_*\overline{\theta}}{kg\theta_*}, \quad (8)$$

$$u_2 - u_1 = \frac{u_*}{k}\left[\ln\left(\frac{z_1}{z_2}\right) - \psi_m\left(\frac{z_2}{L}\right) + \psi_m\left(\frac{z_1}{L}\right)\right], \quad (9)$$

$$\theta_2 - \theta_1 = \frac{\theta_*}{k}\left[\ln\left(\frac{z_1}{z_2}\right) - \psi_h\left(\frac{z_2}{L}\right) + \psi_h\left(\frac{z_1}{L}\right)\right]. \quad (10)$$

Eqs. (6) and (7) are used to calculate u_* and θ_* under neutral condition, which are then taken as the first guess for iteration of eqs. (8)–(10). Eventually u_*, θ_* and L can be determined after repetitive iterations.

Based on the above results, three statistical methods are applied to calculate surface roughness length z_{0m}:

(a) Independent method. The relationship between the dimensionless wind velocity $\kappa u/u_*$ and stability parameter z/L is identified in the log-log coordinate to determine the value of $\kappa u/u_*$ under neutral condition, which is then used in the wind profile equation to obtain the value of z_{0m} (z_{0m}_I).

(b) Optimal method. Using the available values of variables u, d, z/L and u_* during a specific time period, we can solve eq. (1) to obtain the value of z_{0m}. Apparently the value of z_{0m} cannot be identical due to differences in weather conditions and instruments, etc. Therefore, the value that occurs most frequently is taken as the value of z_{0m} (z_{0m}_O) for the specific time period.

(c) Statistical fitting method. Giving an initial guess of z_{0m} and the Obukhov length, eq. (1) can be solved to obtain u. The above method is repeated over a specific time period (1-month in the present study). Correlation coefficients between the solution (u) of the equation and observations are then calculated. The value of z_{0m} that yields the solutions of u that has the highest correlation coefficient with observations is taken as the average z_{0m} (z_{0m}_F) during this specific time period.

The excess resistance κB^{-1} can be derived from field measurements of sensible heat flux, wind speed, and temperature and calculated fluxes that take into account the aerodynamic resistance (Feng et al., 2012). In the practical application, κB^{-1} is often derived from parameterization scheme and applied for sensible heat flux calculation. Beljaars et al. (1991) argued that z_{0m} and z_{0h} are different and showed their difference by $\kappa B^{-1} = \ln(z_{0m} / z_{0h})$. Garratt and Francey (1978) suggested that $\kappa B^{-1} = 2$ for the surface with a single homogeneous vegetation type, but the value will increase (decrease) with the vegetation cover becoming denser (sparser). Sun (1999) found that κB^{-1} in the grassland surface demonstrates a diurnal variation feature. A previous study (Brutsaert, 1982) suggested that the change in κB^{-1} is actually a function of Reynold number (Re_*). So far many parameterization schemes related to Re_* have been developed. Based on measurements in the Tibetan Plateau, Yang et al. (2002) developed a scheme that can well simulate the value of κB^{-1} and its diurnal variation for bare soil surface.

In order to estimate κB^{-1}, we need to first give the equation for sensible heat flux calculation, which is expressed as (Verhoef et al., 1997):

$$H_s = \frac{\rho C_p (T_s - T_a)}{r_h}, \quad (11)$$

where,

$$r_h = \frac{1}{\kappa u_*}\left[\ln\frac{z_m - d}{z_{0m}} + \ln\frac{z_{0m}}{z_{0h}} - \psi_h(\zeta)\right], \quad (12)$$

ρ is the air density (kg / m^3); C_p is the specific heat capacity at constant pressure, here C_p = 1004 J / (kg K); T_s and T_a are surface and air temperature respectively (°C); $\psi_h(\zeta)$ is the stability correction function for temperature, which can be written as (Dyer, 1974):

$$\begin{cases}\psi_h(\zeta) = 2\ln(\dfrac{1+x^2}{2}), & \zeta < 0,\\ \psi_h(\zeta) = -5\zeta, & \zeta > 0.\end{cases} \quad (13)$$

According to the Stefan-Boltzmann law, surface temperature can be derived from the long-wave radiation flux:

$$L^{\uparrow} = (1-\varepsilon_s)L^{\downarrow} + \varepsilon_s\sigma T_s^4, \quad (14)$$

where $L^{\uparrow}$ is outgoing long-wave radiation flux; $L^{\downarrow}$ is incoming long-wave radiation flux; emissivity ε_s is a physical feature of the surface characteristics, which varies with the changes in color and humidity of the surface (Zhang et al., 2010). In the present study, ε_s = 0.95, σ is the Stefan-Boltzmann constant, which is equal to 5.67×10^{-8} W m^{-2} K^{-4}.

The equation for calculation of κB^{-1} can be derived from eqs. (11)–(13), written as:

$$\kappa B^{-1} = \ln\frac{z_{0m}}{z_{0h}} = \frac{\kappa u_*(T_s - T_a)}{H_{\text{obs}}/\rho C_p} - \left[\ln\frac{z_m - d}{z_{0m}} - \psi_h(\zeta)\right]. \quad (15)$$

The parameterization scheme to estimate κB^{-1} in the present study uses the methods described by Yang (2008). Yang's method was developed based on the comparison of seven different schemes with measurements in bare soil surface and/or in low-height grassland as input (Table 1). Note that in both Yuzhong Station and the degraded grassland site of Tongyu Station, the surface is covered by low-height grass and plants, while the farmland site of Tongyu Station is bare soil surface during non-growing season. The parameterization scheme of κB^{-1} is appropriate for application in such kinds of surface. Considering the uncertainty in the κB^{-1} parameterization schemes (Zeng, 2012), it is also applied to the farmland site of Tongyu Station despite the fact that the vegetation at this site is relatively high during the growing season.

2.3 Introduction of the land surface model

In order to verify the effects of the above parameters and scheme in land surface model simulation, the Common Land Model (hereafter CoLM, Dai et al., 2003) is utilized to simulate the sensible heat flux using the original parameters/scheme and the revised parameters/scheme described above. The results are compared to investigate the impact of these new parameters and scheme proposed in the present study. CoLM is a popular land surface model that is widely used in the world. It has been developed on the basis of Land Surface Model (LSM, Bonan, 1995), Biosphere-Atmosphere Transfer Model (BATS, Dickinson et al., 1993), and Institute of Atmospheric Physics Land Surface Model (IAP94, Dai et al., 1997), but with extra modules to describe glacier physics, lake and wetland physics, and dynamic vegetation process. Currently CoLM has been coupled with various climate models and widely applied for studies of land surface processes (Song et al., 2008, 2009).

The USGS land use type and specific parameters are adopted in CoLM. The value of z_{0m} is prescribed for each individual land use type and modified based on the vegetation fraction at each grid box. However, the value of z_{0m} descried in the model is quite different from the true value in the semi-arid region of North China. In addition, the vegetation fraction information used in the model is not accurate. As a result, there exist large biases in the value of z_{0m} and its seasonal variability in the model. For the excess resistance κB^{-1}, the Z98 scheme is used as the default option in CoLM (Zeng et al., 1998).

Table 1 List of different parameterization schemes for κB^{-1} a)

	Reference	Abbreviation
$\kappa B^{-1} = \ln(\text{Pr}\times \text{Re}_*)$	Sheppard (1958)	S58
$\kappa B^{-1} = \kappa\alpha(8\,\text{Re}_*)^{0.45}\,\text{Pr}^{0.8}$	Owen and Thomson (1963)	OT63
$\kappa B^{-1} = 2.46\,\text{Re}_*^{0.25} - 2$	Brutsaert (1982)	B82
$\kappa B^{-1} = 0.1\,\text{Re}_*^{0.5}$	Zilitinkevich (1995)	Z95
$\kappa B^{-1} = 0.13\,\text{Re}_*^{0.45}$	Zeng and Dickinson (1998)	Z98
$\kappa B^{-1} = 1.29\,\text{Re}_*^{0.25} - 2$	Kanda et al. (2007)	K07
$z_{0h} = (70\nu/u_*)\times\exp(-\beta u_*^{0.5}\lvert T_*\rvert^{0.25})$	Yang et al. (2007)	Y07

a) $\text{Re}_* = z_{0m}u_*/\nu$, Pr = 0.71, κ = 0.4, ν is viscosity coefficient α = 0.52 (OT63 and Z98), β = 7.2 (Y07) (Yang et al., 2008).

3. Analysis of results

3.1 Estimation of surface roughness length based on station observations and its characteristic changes

The three methods that are used to estimate z_{0m} are all statistical methods, which can reflect the statistical features of various aspects of the samples. The value of z_{0m} estimated by the three methods can well reflect its seasonal and inter-annual variability and change, although there exist slight differences in the estimated value (Figure 2). Note that the plant growth is quite uniform in the farmland due to the influence of human activity, leading to a consistent estimation of z_{0m} with all the three methods. In contrast, significant differences are found in the estimation of z_{0m} for the two types of grassland surface using the three methods. For the degraded grassland site of Tongyu Station during the period 2003–2007 and for the grassland of Yuzhong Station over most of the time, z_{0m}_O is underestimated while z_{0m}_F is overestimated. In the present study, the average of the estimated values calculated by the three methods is taken for further study. The average value is supposed to maintain the general features of z_{0m} variability and change, and reduces the possible differences caused by different statistical features.

For the three types of surface, plant growth all depends on rainfall. The only exception is the farmland, which is slightly irrigated during the sowing period in drought years. As an important parameter in the vegetation ecology, the value of z_{0m} is mainly dependent on the average height and distribution of surface roughness elements. Hence, the inter-annual variability of z_{0m} corresponds to the inter-annual variability of rainfall, which is especially distinct at the farmland site of Tongyu Station, where the plant is relatively high with large inter-annual variability. Figure 2 also reveals a significant seasonal variability in z_{0m}, which has a large value in the growing season due to the rapid growth of crops in the farmland in semi-arid regions. The value of z_{0m} for the farmland site of Tongyu Station ranges between 85×10^{-3}–153×10^{-3} m during the growing season, while it ranges between 5.1×10^{-3}–9.5×10^{-3} m in the non-growing season. Apparently there is a large seasonal difference in z_{0m} for the farmland site. For the grassland sites, the range of

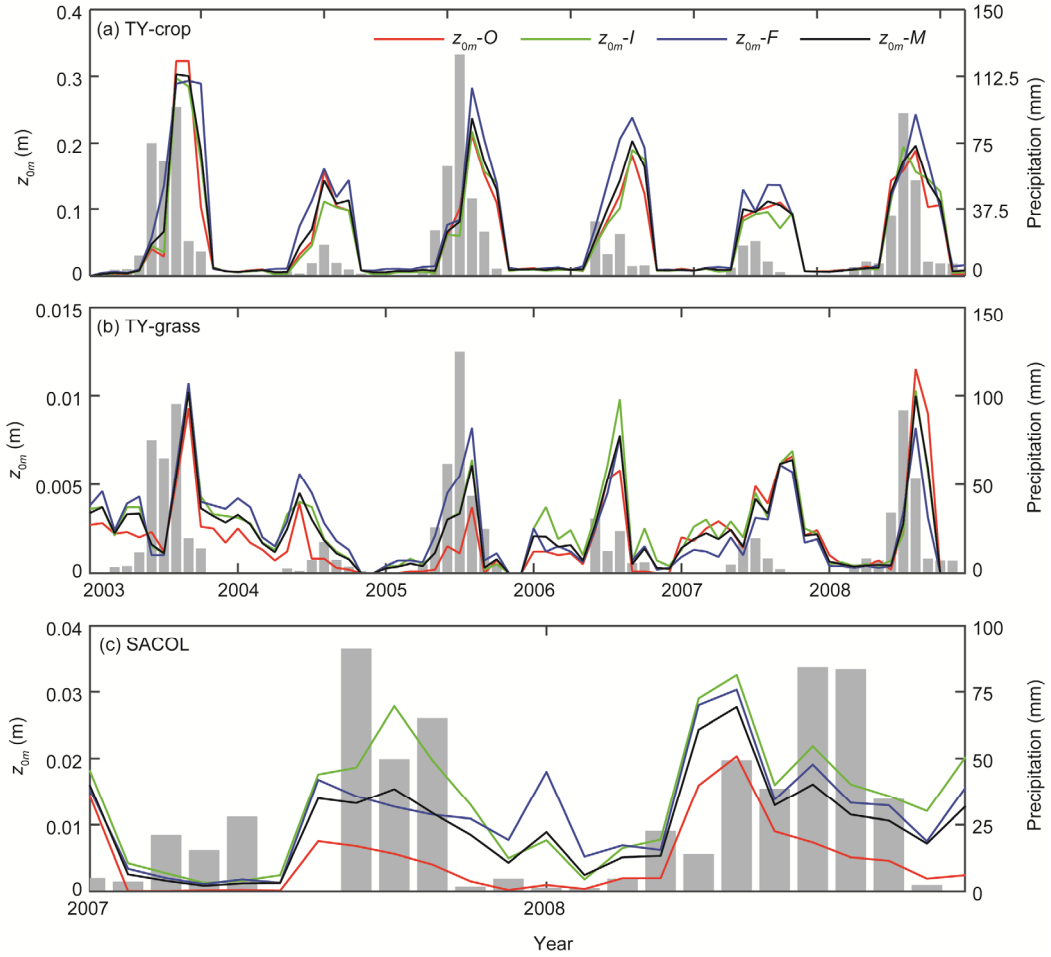

Figure 2 The value of z_{0m} estimated by the three methods (curve lines) and monthly precipitation (histogram). (a) TY-crop: farmland site of Tongyu Station; (b) TY-grass: degraded grassland site of Tongyu Station; (c) SACOL: Yuzhong Station (the same hereinafter). z_{0m}_O: optimal parameter method; z_{0m}_I: independent method; z_{0m}_F: statistical fitting method; z_{0m}_M: average of three methods.

z_{0m} is 1.4×10^{-3}–3.7×10^{-3} m for the degraded grassland site of Tongyu Station and it is 7.4×10^{-3}–11.9×10^{-3} m for the grassland of Yuzhong Station.

3.2 Analysis of characteristic changes of κB^{-1}

κB^{-1} is an important parameter for the calculation of aerodynamic resistance in the surface. With the available value of z_{0m} described previously, κB^{-1} can be calculated from eq. (15). Figure 3 shows the multi-year seasonal and annual averages of diurnal variation of κB^{-1} for the three types of surface. One significant feature is that κB^{-1} demonstrates a distinct diurnal variation with the smallest value occurring in the nighttime. It increases rapidly after the sunrise and remains stable during the daytime, and decreases quickly after the sunset. Looking at the value of κB^{-1} at different seasons, it is the smallest in the winter for all the three types of the surface. The largest value is found at the farmland site of Tongyu Station in the summer and autumn, corresponding to maximum plant growth season. The seasonal variation of κB^{-1} in the degraded grassland site of Tongyu Station and in the grassland site of Yuzhong Station is not as distinct as that in the farmland site. The largest value of z_{0m} appears in the spring and summer at the grassland sites. Molecular diffusion and pressure perturbation are two reasons for the surface-atmosphere momentum transfer, while molecular diffusion controls the transfer of heat. The height and distribution of surface roughness elements impose significant impacts on the momentum transfer via the drag force (Mahrt, 1996). Yang (2008) compared measurements at multiple stations and found no significant difference in the daytime average of z_{0h}. Hence, the value of z_{0m} in the growing season at the farmland site of Tongyu Station is distinctly larger than that of z_{0m} at the degraded grassland site of Tongyu Station and grassland site of Yuzhong Station. It is also larger than that in the non-growing season at the farmland site of Tongyu Station. As a result, the value of κB^{-1} is also larger in the farmland site of Tongyu Station than in other sites during the growing season.

The negative value during the nighttime shown in Figure 3 indicates that the efficiency for heat transfer is larger than that for momentum transfer, which suggests that z_{0h} is larger than z_{0m}. This is quite different from the traditional point of view that momentum transfer efficiency is always larger. Mahrt (1996) argued that the inhomogeneity in the surface may result in domain-average upward momentum transfer that is attributed to the large upward momentum flux over a certain areas within the domain, despite the fact that the domain-average stratification is stable. Yang et al. (2008) proposed that the negative value of κB^{-1} is attributed to inactive eddy activities in the external boundary layer. Hong et al. (2004) found that the inactive eddy activities in the external boundary layer do not affect momentum flux, but can make the calculated heat flux deviate from the prediction based on the similarity theory.

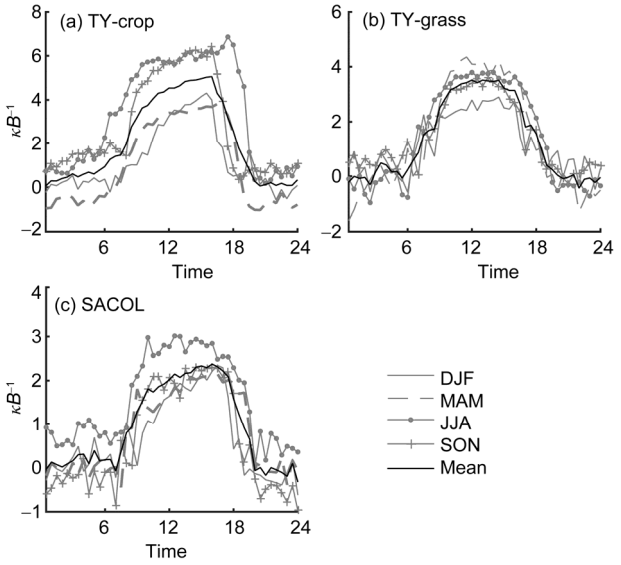

Figure 3 Multi-year seasonal and annual average diurnal variation of at Tongyu staion farmland (a), degraded grassland (b), and Yuzhong Station (c).

The vegetation condition in the grassland and degraded grassland in semi-arid regions is largely controlled by natural factors such as rainfall and temperature, etc. Although there exists large inter-annual variability, the multi-year average results can still demonstrate the feature of larger values in the growing season than that in the non-growing season (Figure 4). During the growing season, the value of κB^{-1} ranges between 2.4–4.0 and 1.4–2.8 for the two types of surface respectively, while ranges between 1.7–3.4 and 1.2–1.9 during the non-growing season (Table 2). Similar to the variation features of z_{0m}, the seasonal variability of κB^{-1} value doesn't show large inter-annual changes. This is because plant growth in the farmland is under the influence of human activity with a relatively fixed schedule of sowing and harvesting. Generally, the value of κB^{-1} gradually increases in the growing season since May when crops begin to germinate, and can reach up to 8.94. After crop harvest in October, the value of κB^{-1} decreases rapidly. The average value of κB^{-1} is 2.72 during the non-growing season.

How to select a reasonable parameterization scheme for κB^{-1} has always been a research focus in land surface model development. In the present study, the performances of seven parameterization schemes in the simulation of κB^{-1} for the three types of surface are compared. κB^{-1} is regarded as a function of surface roughness length and friction velocity u_* in all the seven schemes. The exponential and logarithmic z_{0m} forms of input argument $Re_* = z_{0m}u_*/\nu$ are used in fitted equations to obtain the value of κB^{-1}. Due to the difference in experimental data, the fitting coefficients are different in these schemes. In addition to z_{0m} and u_*, the

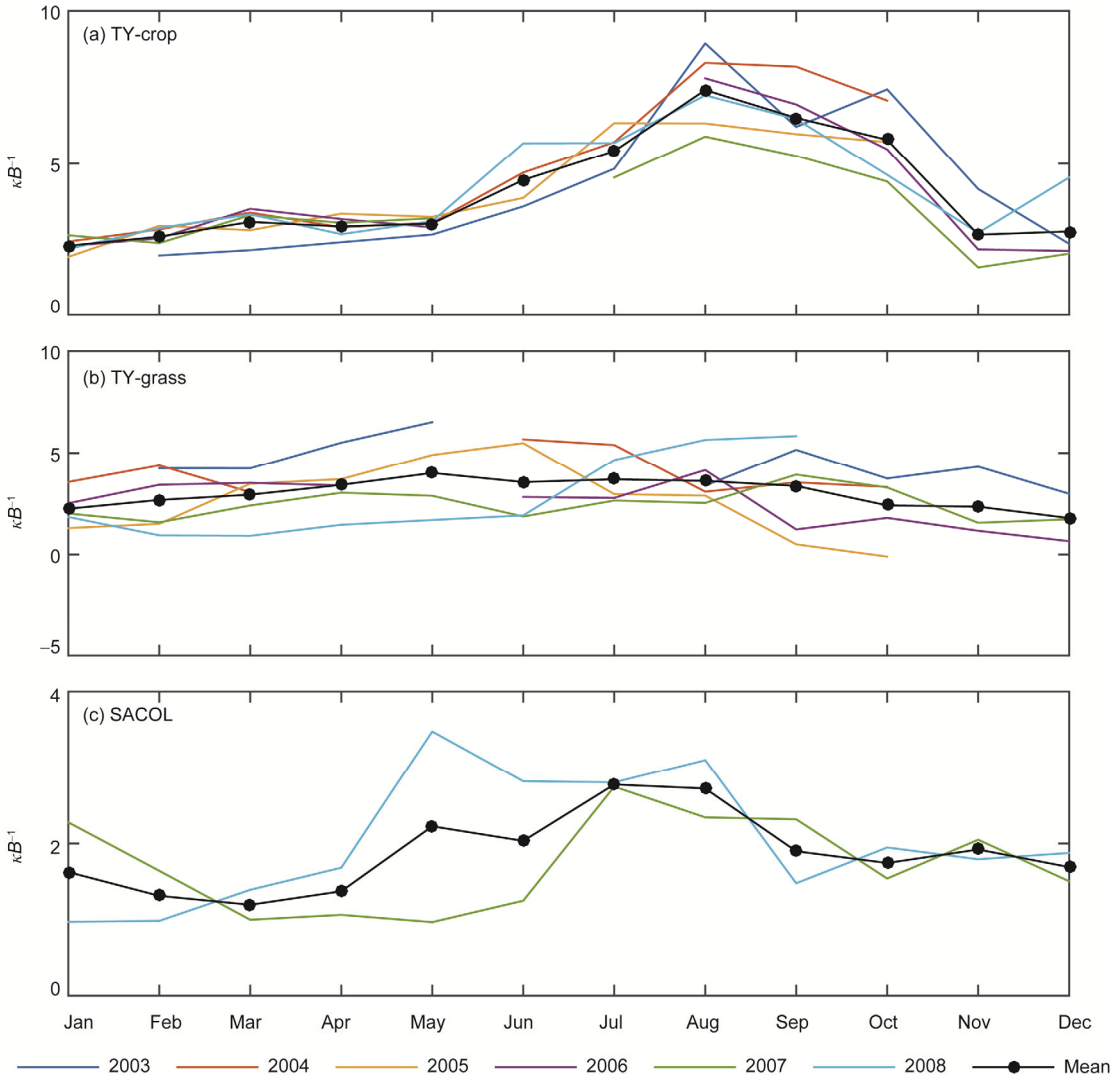

Figure 4 Seasonal variability and inter-annual difference in the value of κB^{-1} for the three types of surface: Tongyu staion farmland (a), degraded grassland (b), and Yuzhong Station (c).

Table 2 Multi-year average monthly value of excess resistance κB^{-1}

Station	Jan	Feb	Mar	Apr	May	Jun	Jul	Aug	Sep	Oct	Nov	Dec
Farmland, Tongyu	2.30	2.60	3.08	2.93	3.03	4.46	5.42	7.42	6.51	5.80	2.66	2.76
Degraded grassland	2.24	2.67	2.93	3.42	4.00	3.55	3.69	3.61	3.36	2.40	2.34	1.78
Grassland, Yuzhong	1.63	1.32	1.20	1.38	2.22	2.03	2.77	2.72	1.90	1.75	1.92	1.69

characteristic temperature T_*, which has a distinct diurnal variation, is introduced into the Y07 scheme. T_* is used as an input argument to calculate z_{0h} which is then used in $\ln(z_{0m}/z_{0h})$ to obtain κB^{-1}. This is an effective approach to reproduce the diurnal variation of κB^{-1}. Since there is a large difference in the surface roughness length between growing and non-growing seasons for the farmland site of Tongyu Station, we consider the growing and non-growing seasons separately.

Figure 5 shows that the S58 and B82 schemes overestimate κB^{-1} and the bias is larger for the surface with larger z_{0m}. Contrarily, the Z95 and Z98 schemes underestimate κB^{-1} and the bias increases when z_{0m} decreases. The performance of K07 and OT64 schemes is quite different for different surface types, indicating an unstable condition for the two schemes. The Y07 scheme performs well with relatively small biases in its simulation. Looking at the diurnal variation simulation, it is found that the Y07 scheme can well reproduce the diurnal variation of κB^{-1}. The Y07 simulations are consistent with observations for the farmland site of Tongyu Station during the non-growing season and for the degraded grassland site of Tongyu and grassland

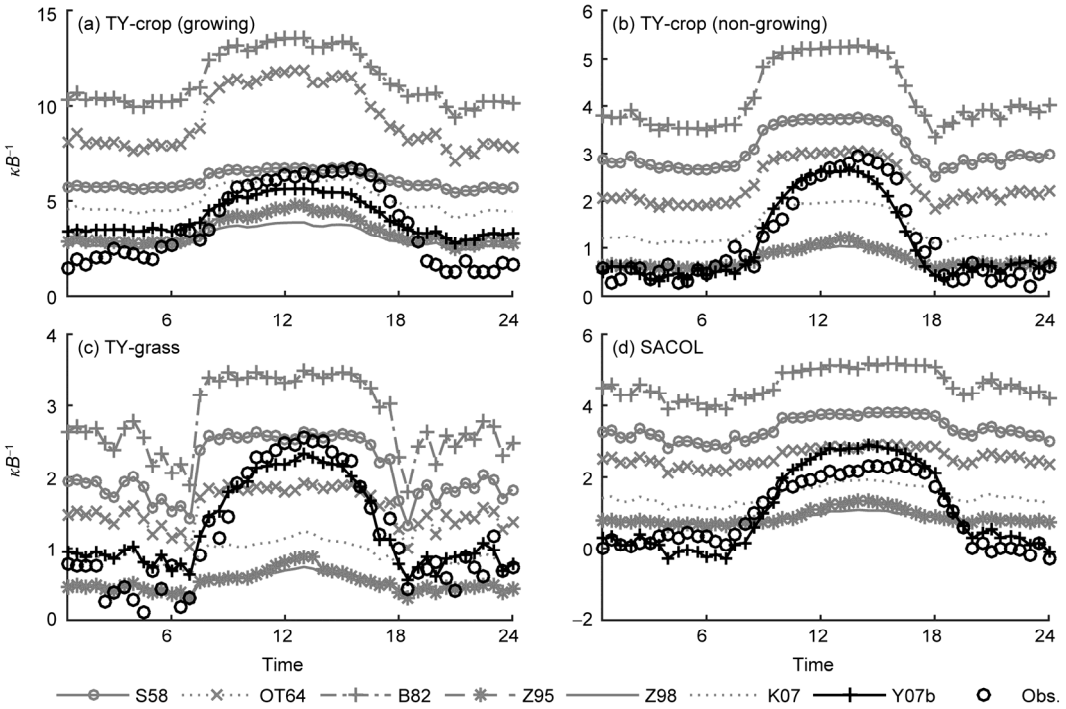

Figure 5 Simulated and observed diurnal variation of κB^{-1}. (a) TY-crop (growing): growing season at the farmland site of Tongyu Station; (b) TY-crop (non-growing): non-growing season at the farmland site of Tpngyu station; (c) TY-grass: degraded grassland site of Tongyu Station; (d) SACOL: Yuzhong Station.

site of Yuzhong, where z_{0m} is relatively small. Meanwhile, for the farmland site of Tongyu Station during the growing season, the performance of all the seven schemes is less satisfactory. Underestimation of κB^{-1} during the daytime and overestimation in the nighttime is a common feature in the simulations, even for those schemes that can yield average values close to observations.

In order to further compare the capability of the seven schemes, we calculate sensible heat flux by eqs. (11) and (12), using the value from the seven schemes. Normalized standard deviations of the difference between the observed and simulated heat flux (NSEE) using the seven schemes are calculated to compare the performance of these schemes (Table 3). The smallest NSEE is found in the K07 simulation for the farmland site of Tongyu Station during the growing season, especially during the months from July to September, when crops grow rapidly and reach their peak height. For the degraded grassland site of Tongyu Station and the grassland site of Yuzhong Station, the Y07 scheme also yields better results than other schemes except for a few months when NESS is the smallest for the OT64 and S58 simulations. Based on the above results, in this study we apply the Y07 scheme in CoLM model to investigate its impact on surface flux simulation.

3.3 Verification of model performance

In order to further verify the impact of these key parameters obtained from field measurements, i.e., surface roughness length z_{0m} and excess resistance, on the improvement of surface flux simulation, a suite of nine experiments (three experiments for each of the three types of surface) has been conducted in the present study. The CoLM is applied to simulate surface fluxes for the farmland site and degraded grassland site of Tongyu Station. The simulation covers the period from October 2003 to October 2004, when continuous and high-quality observations are available at these two sites. The model is also applied for simulation at the Yuzhong Station for the period from October 2007 to October 2008. The simulated surface fluxes with and without changes in the key parameters are compared with observations. The design of experiments is described in detail as follows:

(1) Comparative experiment (EX1): no modification is made for the parameters in the model. The default values of these parameters are used in the experiment, i.e., z_{0m}= 0.1 m, κB^{-1} is adopted from Z98 scheme.

(2) A single parameter optimization experiment (EX2): κB^{-1} remains unchanged, but the default value of z_{0m} is replaced by the value calculated in the present study.

(3) Multi-parameter optimization experiment (EX3): the same as EX2, but the Z98 scheme is replaced by the Y07 scheme.

Root mean square error (*DRMS*), bias, sign change rate (*NSC*), and an overall objective function (criteria) are defined to quantify the difference between the model simula-

Table 3 The scheme that yields best simulation of multi-year average monthly [a)]

	Jan	Feb	Mar	Apr	May	Jun	Jul	Aug	Sep	Oct	Nov	Dec
Farmland, Tongyu	Y07	Y07	Y07	K07	Y07	Y07	K07	K07	K07	Z98	Y07	Y07
Degraded grassland, Tongyu	OT64	Y07	Y07	Y07	Y07	Y07	Y07	Y07	S58	Y07	Y07	Y07
Grassland, Yuzhong	Y07	Y07	Y07	Y07	Y07	Y07	OT64	OT64	Y07	Y07	Y07	Y07

a) Abbreviation for the schemes is given in Table 1. Y07 is the optimal scheme for degraded grassland site of Tongyu and grassland site of Yuzhong as well as for the farmland site of Tongyu Station during the non-growing season.

tions.

The three statistical variables are written as:

$$DRMS(\theta)=\sqrt{\frac{1}{N}\sum_{t}^{N}(q_t^{\mathrm{sim}}(\theta)-q_t^{\mathrm{obs}}(\theta))^2}\ , \tag{16}$$

$$BIAS=\frac{1}{N}\left|\sum_{t}^{N}(q_t^{\mathrm{sim}}(\theta)-q_t^{\mathrm{obs}}(\theta))\right|, \tag{17}$$

$$NSC=\left|\frac{n_1}{n_1+n_2}-0.5\right|, \tag{18}$$

$$criteria(\theta)=\left|\frac{1}{m\left(\sum_{i=1}^{n}w_j\right)}\left(\sum_{i=1}^{n}\left(\sum_{j=1}^{n}w_j f_{i,j}(\theta)\right)\right)\right|, \tag{19}$$

where $q(\theta)$ represents the model output variable (for example, sensible heat flux), sim represents the simulations, obs represents observations, and N is the time step. *NSC* reflects the changing frequency of difference between the simulation and observation. n_1 and n_2 represent the times when observation is larger than simulation and that when simulation is larger than observation, respectively. $n_1+n_2<=N$. $f_{i,j}(\theta)$ represents the sub-criteria factors, which can be *DRMS*, *BIAS*, and/or *NSC*. m is the number of target variables, n is the number of sub-criteria functions, w is the weighting factor for the sub-criteria factors (in the reference for weighting factor determination, i.e., Li (2011), *DRMS*=3, *BIAS*=2, *NSC*=1).

Figure 6 shows the simulated and observed sensible heat flux. Using the surface roughness length estimated from observations, the simulated sensible heat flux becomes more consistent with observations. When the estimated κB^{-1} is then introduced into the model, the simulation is further improved. Specifically, the default value of z_{0m} is quite different from the true value for the farmland site of Tongyu Station during the non-growing season, when the farmland is actually bare soil surface. In the experiment with single parameter optimization, the CoLM simulation is greatly improved. During the growing season that starts in May, accompanied with the plant growth, the default value of z_{0m} becomes close to the observation-based estimated value. This explains why the improvement of CoLM simulation in the experiment with single parameter optimization is not distinct.

The parameterization scheme for κB^{-1} mainly affects sensible heat transfer between the surface and vegetation canopy layer. Therefore, multi-parameter optimization can greatly improve the model performance during the growing season. Field measurements have shown clearly that the estimated value of z_{0m} for the degraded grassland of Tongyu and grassland of Yuzhong is far less than the default value of z_{0m} in the model. This explains why the simulation of sensible heat flux in the single parameter optimization experiment is significantly improved, while the multi-parameter optimization experiment demonstrates further improvements to a certain extent. However, note that the characteristic temperature introduced into the parameterization scheme is an intermediate variable for iteration in the CoLM model. The accumulated errors generated by the exponential calculation can lead to large singular values in the simulation of multi-parameter optimization experiment.

Table 4 lists the distribution of *DRMS*, *BIAS*, and *NSC* based on the simulated sensible heat flux at the three sites of the observation stations. Results for simulations at the farmland site are discussed separately for growing season and non-growing season. Apparently each sub-criteria variable indicates that the simulations in both the single parameter and multi-parameter optimization experiments are better than that without optimization, i.e., only the default value is used in the simulation. The above results indicate that the land surface model can better simulate sensible heat flux if reasonable values of key parameters are used. Compared with the single parameter optimization, multi-parameter optimization results in further decreases in the value of the sub-criteria factors, suggesting that multi-parameter optimization can further improve the model performance in sensible heat flux simulation.

Considering all the sub-criteria factors as a whole, the overall objective functions (criteria) for the three types of surface all decrease after the single parameter and multi-parameter optimizations. Specifically, single parameter optimization significantly decreases the objective function for the farmland site during the non-growing season, for the degraded grassland site of Tongyu Station, and for the grassland of Yuzhong Station. Multi-parameter optimization can further decrease the objective function, although the decrease is not that distinct. However, the magnitude of decrease in the objective function for the farmland site of Tongyu Station during the non-growing season is much larger in the multi-parameter optimization experiment than

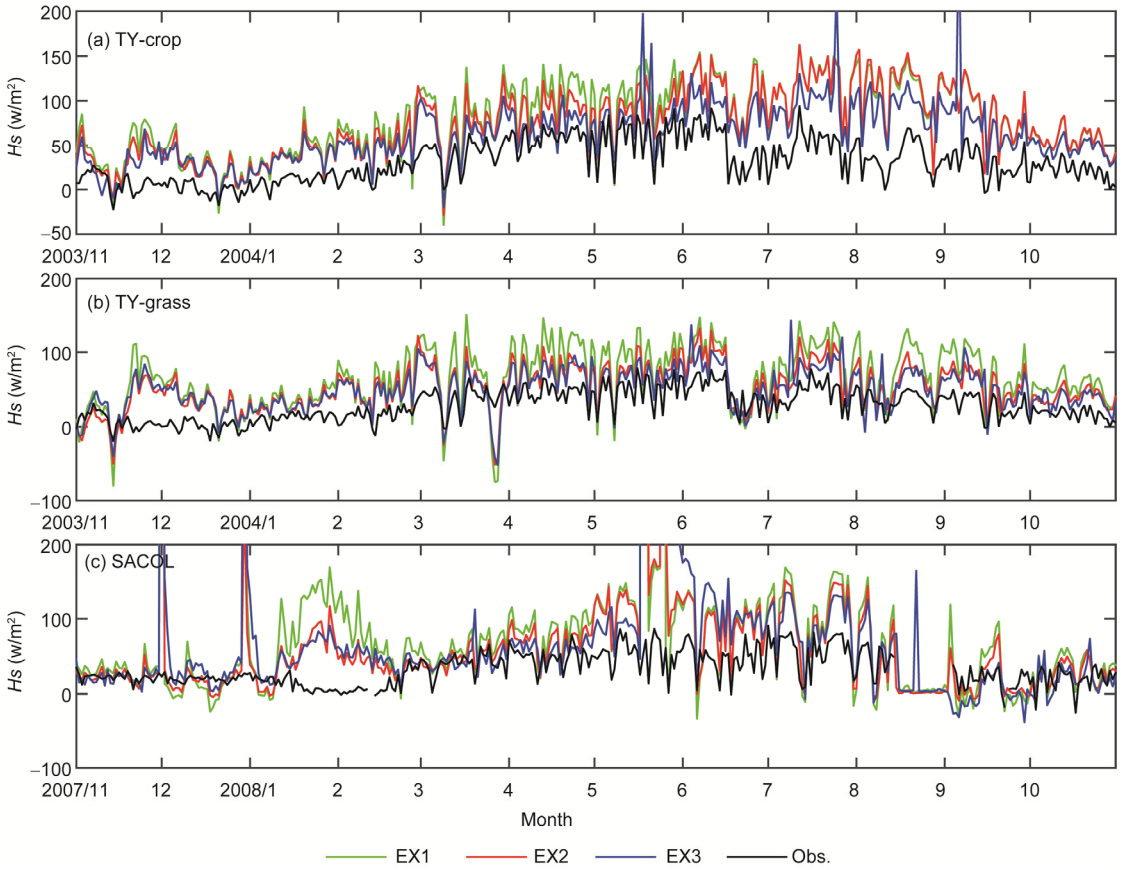

Figure 6 Comparison of simulated and observed sensible heat flux with and without modification of key parameters in the model. (a) Tongyu staion farmland; (b) degraded grassland; (c) Yuzhong Station.

Table 4 The sub-criteria factors and objective functions before and after the changes of key parameters in the model [a)]

	Farmland of Tongyu (non-growing season)				Farmland of Tongyu (growing season)				Degraded grassland				Grassland of Yuzhong			
	DRMS	*BIAS*	*NSC*	*Cri.*	*DRMS*	*BIAS*	*NSC*	*Cri.*	*DRMS*	*BIAS*	*NSC*	*Cri.*	*DRMS*	*BIAS*	*NSC*	*Cri.*
EX1	43.0	37.2	0.48	33.98	60.8	57.0	0.49	49.48	47.0	36.8	0.41	35.84	46.0	26.8	0.27	31.98
EX2	34.2	29.7	0.47	27.08	60.5	55.9	0.50	48.97	32.0	24.3	0.39	24.17	31.1	17.1	0.20	**21.28**
EX3	26.7	22.4	0.45	**20.89**	50.4	39.9	0.46	**38.58**	30.3	21.6	0.39	**22.42**	33.3	16.4	0.21	22.15

a) *Cri.* represents objevtive function (Criteria). The other criteria variables are the same as described in the text. Bold indicates the smallest value of objective function.

that in the single parameter optimization experiment.

The above discussion and quantitative analysis of differences in the simulations with and without parameter optimization clearly indicate that introduction of reasonable values for the key aerodynamic parameters can improve the capability of land surface model for the simulation of surface heat flux. The improvement can be significant for some specific surface types and during certain specific time periods.

4. Discussion and conclusion

In this study, long-term continuous measurements of surface-atmosphere interaction at two observation stations in the semi-arid region of China, Tongyu and Yuzhong, are combined with the planetary boundary layer theory to estimate the value of two key aerodynamic parameters, i.e., surface roughness length z_{0m} and excess resistance κB^{-1}. Multiple parameterization schemes have been used in the study and their results are compared. The retrieved values of these parameters are then introduced in the land surface model to investigate their impact on sensible heat flux. The model performances with and without modification of these parameters are compared. The main conclusions are as follows.

(1) For both grassland and farmland surfaces, the surface roughness length z_{0m} reflects the condition of vegetation

growth. Under natural condition with only slight irritation, vegetation growth to a large extent relies on weather condition such as precipitation. As a result, z_{0m} demonstrates a distinct seasonal and inter-annual variability. Hence, using a fixed value of z_{0m} will result in biases in the calculation of surface-atmosphere fluxes.

(2) Among the seven parameterization schemes used in the present study, the Y07 scheme can better reproduce the diurnal variation of κB^{-1}. Meanwhile, κB^{-1} also demonstrates distinct inter-annual variability due to large inter-annual changes in z_{0m}.

(3) Optimization of parameters and parameterization scheme is an important approach to improve the capability of land surface mode. Parameterization schemes for surface roughness length and κB^{-1} are often developed and verified based on limited measurements at a few observation stations. In the semi-arid region of China, vegetation condition is fragile and highly sensitive to climate and climate change. Surface condition is often complicated and with large spatial-temporal variability. In the present study, the values of several key surface parameters are identified based on field measurements and applied in the land surface model. It is found that the model simulation of sensible heat flux has been greatly improved at surface with low-height vegetation. Meanwhile, modification of the κB^{-1} parameterization scheme has significantly improved the model performance in sensible heat flux simulation for farmland during the growing season.

It should be noted that the present study is based on field measurements and planetary boundary layer flux transfer theory. Optimization of parameters using this method can provide realistic estimation of parameter values that are close to true values in the real world. This method is easy to realize since it can define the objective functions in a relatively flexible way to assess the effects of optimization and to a certain degree can avoid the physical evidence for optimization. However, the approach used in the present study not only emphasizes the physics involved in the optimization, but also provides reliable and realistic estimation of values for several key parameters.

With increases in both field experiments and observation stations, more types of surface will be introduced into the surface-atmosphere interaction study. The method proposed in the present study has the potential to be promoted for further application and can be incorporated into regional climate modeling study. Note that the land surface model describes a series of complicated biophysical/chemical processes that involve the surface, soil, and vegetation etc., and includes numerous parameters. Due to the complexity of the processes involved in land surface modeling study, it is imperative to take advantage of regional remote sensing information and combine this information with optimization methods to better identify values for various parameters in the land model and further improve the capacity of regional climate model. This will be our future research topic.

Acknowledgements *The observations at Tongyu Station and Yuzhong Station are provided by Key Laboratory of Regional Climate-Environment for Temperate East Asia at the Institute of Atmospheric Physics, Chinese Academy of Sciences and Semi-arid Climate Observatory and Laboratory at Lanzhou University (SACOL), respectively. The authors appreciate Professor Yongkang Xue from the University of California, Los Angeles for his valuable advices. This work was supported by the National Basic Research Program of China (Grant No. 2011CB952002), the National Natural Science Foundation of China (Grant Nos. 41475063, 41005047), Program for New Century Excellent Talents in University, and the Jiangsu Collaborative Innovation Center for Climate Change.*

References

Beljaars A C M, Holtslag A A M. 1991. Flux parameterization over land surface for atmospheric models. J Appl Meteorol, 30: 327–341

Bonan G B. 1996. A land surface model (LSM Version 1.0) for ecological, hydrological, and atmospheric studies: Technical description and user's guide. NCAR Tech. Note NCAR/TN-417+STR

Brutsaert W. 1982. Evaporation into the Atmosphere: Theory, History, and Applications. Boston: Kluwer Academic Publishers. 299

Chen J Y, Wang J M, Guang T N. 1997. An independent method to determine the surface roughness length (in Chinese). Chin J Atmos Sci, 17: 21–26

Chen Y Y, Yang K, Zhou D G, Qin J, Guo X F. 2010. Improving the Noah land surface model in arid regions with an appropriate parameterization of the thermal roughness length. J Hydrometeorol, 11: 995–1006

Dai Y J, Zeng Q C. 1997. A land surface model (IAP94) for climate studies part I: Formulation and validation in off-line experiments. Adv Atmos Sci, 14: 433–433

Dai Y J, Zeng X B, Dickinson R E, Baker I, Bonan G B, Denning A S, Dirmeyer P A, Houser P R, Niu G Y, Oleson K W, Schlooser C A, Yang Z L. 2003. The common land model. Bull Amer Meteorol Soc, 84: 1013–1023

Dan L, Fu C B, Wu J. 2011. Spatial and temporal characteristics of global sensible and latent heat fluxes simulated by a two-way land-air coupled model (in Chinese). Climatic Environ Res, 16: 113–125

Dickinson R E, Kennedy P J, Henderson-Sellers A. 1993. Biosphere-atmosphere transfer scheme (BATS) version 1e as coupled to the NCAR community climate model. NCAR Techn. Note-378+STR.

Dyer A J. 1974. A review of flux-profile relationships. Bound-Layer Meteor, 7: 363–372

Feng J M, Fu C B. 2007. Inter-comparison of long-term simulations of temperature and precipitation over China by different regional climate models (in Chinese). Chin J Atmos Sci, 5: 805–814

Feng J W, Liu H Z, Wang L. 2012. Seasonal and inter-annual variation of surface roughness length and bulk transfer coefficients in semiarid area. Sci China Earth Sci, 55: 254–261

Foken T, Göockede M, Mauder M, Mahrt L, Amiro B, Munger W. 2005. Post-field data quality control. In: Lee X, Massman W, Law B, eds. Handbook of Micrometeorology. Heidelberg: Springer. 181–208

Fu C B, An Z S, Guo W D. 2005. Evolution of life-supporting environment in our nation and the predictive study of aridification in Northern China (II): Scientific innovations and its conteribution to national demands (in Chinese). Adv Earth Sci, 20: 1168–1175

Fu C B, Guo W D. 2008. Regional Climate of China. Heidelberg: Springer. 155–217

Fu C B, Wang S Y, Xiong Z, Gutowski W J, Lee D K, McGregor J L, Sato Y, Kato H, Kim J W, Suh M S. 2005. Regional climate model intercomparison project for Asia. Bull Amer Meteorol Soc, 86: 257–266

Fu C B, Weng G. 2002. Several issues on aridification in the Northern China (in Chinese). Climatic Environ Res, 7: 22–29

Gao Z Q, Bian L G, Lu C G. 2002. Estimation of aerodynamic parameters in urban areas (in Chinese). Quart J Appl Meteor, 13: 26–33

Garratt J, Francey R. 1978. Bulk characteristics of heat transfer in the unstable, baroclinic atmospheric boundary layer. Bound-Layer Meteor, 15: 399–421

Guan X D, Guo N, Huang J P. 2008. Applicability analysis of VCI to monitoring Northwest China drought (in Chinese). Plateau Meteor, 27: 1046–1053

Guan X D, Huang J P, Guo N, Bi J R, Wang G Y. 2009. Variability of soil moisture and its relationship with surface albedo and soil thermal parameters over the Loess Plateau. Adv Atmos Sci, 26: 692–700
Huang J P, Zhang W, Zuo J Q, Bi J R, Shi J S, Wang X, Chang Z L, Huang Z W, Yang S, Zhang B D, Wang G Y, Feng G H, Yuan J Y, Zhang L, Zuo H C, Wang S G, Fu C B, Chou J F. 2008. An overview of the semi-arid climate and environment research observatory over the Loess Plateau. Adv Atmos Sci, 25: 906–921
Kanda M, Kanega M, Kawai T, Morwaki R, Sugawara H. 2007. Roughness lengths for momentum and heat derived from outdoor urban scale models. J Appl Meteorol Climatol, 46: 1067–1079
Li H Q, Guo W D, Sun G D. 2011. A new approch for parameter optimization in land surface model. Adv Atmos Sci, 28: 1056–1066
Ling X L, Guo W D, Zhao Q F, Sun Y L, Zou Y H, Hu Z H, Fu C B. 2012. Evaluating CEOP model performance in semi-arid region of China. Environ Res Lett, 7: 025202, doi: 10.1088/1748-9326/7/2/025202
Liu H Z, Dong W J, Fu C B, Shi L Q. 2004. The long-term field experiment on aridification and the ordered human activity in semi-arid area at Tongyu, Northeast China (in Chinese). Climatic Environ Res, 9: 378–389
Liu J, Arndt C, Hertel T W. 2004. Parameter estimation and measures of fit in a global, general equilibrium model. J Econ Integr, 19: 626–649
Liu S H, Chen H S. 1993. Comparison of the turbulent flux indirect calculation method in the atmosphere surface layer (in Chinese). Acta Scienti Natura Uni Pekinensis, 29: 615–621
Liu Y Q, He Q, Zhang H S, Mamtimin A. 2012. Improving the CoLM in Taklimakan Desert hinterland with accurate key parameters and an appropriate parameterization scheme. Adv Atmos Sci, 29: 381–390
Ma Y M, Menenti M, Feddes R, Wang J M. 2008. Analysis of the land surface heterogeneity and its impact on atmospheric variables and the aerodynamic and thermodynamic roughness lengths. J Geophys Res, 113: D08113, doi: 10.1029/2007JD009124
Ma Z G, Fu C B. 2003. Interannual characteristics of the surface hydrological variables over the arid and semi-arid areas of northern China. Glob Planet Change, 37: 189–200
Ma Z G, Fu C B. 2005. Decadal variations of arid and semi-arid boundary in China (in Chinese). Chin J Geophy, 48: 519–525
Mahrt L. 1996. The bulk aerodynamic fomulation over heterogeneous surfaces. Bound-Layer Meteor, 78: 87–119
Moore C. 1986. Frequency response corrections for eddy correlation systems. Bound-Layer Meteor, 37: 17–35
Owen P R, Thomson W R. 1963. Heat transfer across rough surface. J Fluid Mech, 15: 321–334
Pitman A J. 2003. The evolution of, and revolution in, land surface schemes designed for climate models. Int J Climatol, 23: 479–510
Prueger J H, Kustas W P, Hipps L E, Hatfield J L. 2004. Aerodynamic parameters and sensible heat flux estimates for a semi-arid ecosystem. J Arid Environ, 57: 87–100
Qiu Y J, Wu F J, Liu Z. 2010. Problem of the Gradient Method to Study Aerodynamic Roughness (in Chinese). Transac Atmos Sci, 33: 697–702
Sheppard P A. 1958. Transfer across the earth's surface and through the air above. Q J R Meteorol Soc, 84: 205–224
Song Y M, Guo W D, Zhang Y C. 2008. Simulation of latent heat flux exchange between land surface and atmosphere in temperate mixed forest and subtropical artificial coniferous forest sites in China by CoLM (in Chinese). Plateau Meteor, 27: 967–977
Song Y M, Guo W D, Zhang Y C. 2009. Performances of CoLM and NCAR_CLM3.0 in simulating land-atmosphere interactions over typical forest ecosystems in China part II. Impact of different parameterization schemes on simulations (in Chinese). Climatic Environ Res, 14: 243–257
Sun J. 1999. Diurnal variations of thermal roughness height over a grassland. Bound-Layer Meteor, 92: 407–427
Sun S F. 2005. Physical, Biochemical Mechanism and Parameter Schemes in Land Surface Process (in Chinese). Beijing: Meteorological Press. 307
Takagi K, Miyata A, Harazono Y, Ota N, Komine M, Yoshimoto M. 2003. An alternative approach to determining zero-plane displacement, and its application to a lotus paddy field. Agric Meteorol, 115: 173–181
Tu G, Liu H Z, Dong W J. 2009. Characteristics of the surface turbulent fluxes over degraded grassland and cropland in the semi-arid area (in Chinese). Chin J Atmos Sci, 33: 719–725
Verhoef A, Allen S J, Lloyd C R. 1999. Seasonal variation of surface energy balance over two Sahelian surfaces. Int J Climatol, 19: 1267–1277
Verhoef A, DeBruin H A R, VandenHurk B. 1997. Some practical notes on the parameter kB-1 for sparse vegetation. J Appl Meteorol, 36: 560–572
Wang G Y, Huang J P, Guo W D, Zuo J Q, Wang J M, Bi J R, Huang Z W, Shi J S. 2010. Observation analysis of land-atmosphere interactions over the Loess Plateau of northwest China. J Geophys Res, 115: D00K17, doi: 10.1029/2009JD013372
Webb E K, Pearman G I, Leuning R. 1980. Correction of flux measurements for density effects due to heat and water vapour transfer. Q J R Meteorol Soc, 106: 85–100
Wieringa J. 1993. Representative roughness parameters for homogeneous. Bound-Layer Meteor, 63: 323–363
Wilczak J M, Oncley S P, Stage S A. 2001. Sonic anemometer tilt correction algorithms. Bound-Layer Meteor, 99: 127–150
Wu J K, Ding Y J, Shen Y P, Wang G X. 2006. Energy balance in the irrigational intercropping field in the middle reaches of Heihe River. J Glaciol Geocry, 28: 443–449
Yang K, Koike T, Fujii H, Tamagawa K, Hirose N. 2002. Improvement of surface flux parametrizations with a turbulence-related length. Q J R Meteorol Soc, 128: 2073–2087
Yang K, Koike T, Ishikawa H, Kim J, Li X, Liu H Z, Liu S M, Ma Y M, Wang J M. 2008. Turbulent flux transfer over bare-soil surfaces: Characteristics and parameterization. J Appl Meteorol Climatol, 47: 276–290
Yang K, Watanabe T, Koike T, Li X, Fuji H, Tamagawa K, Ma Y M, Ishikawa H. 2007. Auto-calibration system developed to assimilate AMSR-E data into a land surface model for estimating soil moisture and the surface energy budget. J Meteorol Soc Jpn, 85: 229–242
Yao Y H, Guo W D, Song Y M. 2010. Evaluating CEOP model performance with the observational data from Tongyu reference site, semi-arid region of China. Asia-Pacific J Atmos Sci, 46: 475–481
Zeng X B, Dickinson R E. 1998. Effect of surface sublayer on surface skin temperature and fluxes. J Clim, 11: 537–550
Zeng X B, Wang Z, Wang A H. 2012. Surface skin temperature and the interplay between sensible and ground heat fluxes over arid regions. J Hydrometeorol, 13: 1359–1370
Zhang P Y, Jiang L M, Qiu Y B. 2010. Study of the Microwave Emissivity Characteristics over Different Land Cover Types (in Chinese). Spectro Spectral Anal, 6: 1446–1451
Zhang Q, Lü S H. 2003. The determination of roughness length over city surface (in Chinese). Plateau Meteor, 22: 24–32
Zhang W Y, Zhang Y, Lu X J, Guo Z H, Wang X Y. 2009. Analysis on heterogeneous underlying surface roughness length in semi-arid mountains area of Loess Plateau, China (in Chinese). Plateau Meteor, 28: 763–768
Zhang Y, Lü S H, Chen S Q, Ao Y H, Hu Z Y, Wei Z G. 2005. Characteristics of energy budget and microclimate on the edge of oasis Summer (in Chinese). Plateau Meteor, 24: 527–533
Zheng D H, Velde R V D, Su Z B, Booij M J, Hoekstra A Y, Wen J. 2014. Assessment of roughness length schemes implemented within the Noah Land Surface Model for high-altitude regions. J Hydrometerorol, 15: 921–937
Zheng W Z, Wei H L, Wang Z, Zeng X B, Meng J, Ek M, Mitchell K, Derber J. 2012. Improvement of daytime land surface skin temperature over arid regions in the NCEP GFS model and its impact on satellite data assimilation. J Geophys Res, 117: D06117, doi: 10.1029/2011JD015901
Zhong Z, Su B K, Zhao M. 2002. A new method to determin effective roughness length in atmospheric model (in Chinese). Prog Nat Sci, 12: 519–523
Zhou Y L, Sun X M. Zhu Z L, Wen X F, Tian J, Zhang R H. 2007. Comparative research on four typical surface roughness length calculation methods (in Chinese). Geogra Res, 26: 887–896
Zilitinkevich S. 1995. Non-local turbulent transport pollution dispersion aspects of coherent structure of convective flows. In: Power H, Moussiopoulos N, Brebbia C A, eds. Air Pollution III, Air Pollution Theory and Simulation. Boston: Computational Mechanics Publication. 53–60